Magnetoglobus multicellularis Form Active Crystals when Confined to a Surface with an Applied Magnetic Field

Alejandra Rosselli-Calderon

Clark University Department of Physics

(Dated: May 8, 2020)

Abstract

Multicellular Magnetotactic Bacteria (MMB) live in spherical colonies composed of 10-40 individual bacteria. These bacteria are the only known obligately multicellular bacteria. The colony swims as a single unit parallel to the Earth's magnetic field. When an imposed magnetic field is oriented normal to a glass surface, aggregates accumulate into a monolayer on the glass surface. As the magnitude of magnetic field increases, the density of the colonies increases and the cells are more strongly confined to the glass surface. At a critical field strength, the mean free path of the colonies shrinks to the radius of a single colony. The colonies display a crystalline packing. Unlike previous examples of active crystals (e.g., with colloids and fast swimming bacteria), these bacteria spontaneously detach and reincorporate into the structure at rates dependent on the strength of the applied field.

INTRODUCTION

Magnetoglobus multicellularis is a species of magnetotactic multi-cellular bacteria of the class Deltaproteobacteria. They live in colonies consisting of 10-40 individual magnetotactic cells which are organized in a spherical or ovoloid way [1]. In Figure 1 we can see the shape of the colonies and the distribution of individual cells within a colony. These organisms can be found in microaerobic and anaerobic habitats, with a higher density at the interface between oxic and anoxic environments [2]. MMB are characterised by the synthesis of magnetic iron crystals, called magnetosomes. These magnetosomes can be either iron oxide magnetite (Fe_3O_4) or iron sulphide greigite (Fe_3S_4) [3]. In Figure 1, on the left, the red rectangle shows the location of one of these magnetosomes in an MMB.

Magnetosomes create a magnetic dipole moment in each bacteria colony. The magnetic dipole moment causes the colony to align with the local magnetic fields. The right image on Figure 1 shows how the MMB align when the imposed magnetic field is changed in direction. The presence of flagella in these bacteria allows them to propel themselves based on this orientation [1]. This process is known as magnetotaxis and it is a combination of a colony's passive alignment with the magnetic field and the propulsion by using flagella to swim. The magnetotactic bacteria colonies are not pulled to the geomagnetic poles of the Earth [4].

The MMB used throughout this experiment were collected from a marsh in Falmouth, Massachusetts, United States (41°34'34.2"N 70°38'21.4"W). They were then magnetically

concentrated with neodymium magnets and purified again by sampling from areas with a higher magnetic field.

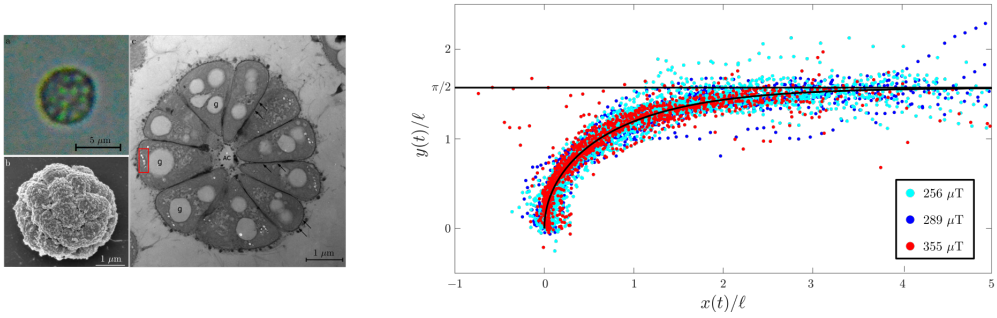

FIG. 1: Image of *Magnetobulus multicellularis* under different microscopes (left). Alignment of *Magnetobulus multicellularis* with different magnetic fields due to their magnetic dipole moment (right)

MATERIALS & METHODS

Sampling MMB

The MMB have not been cultivated in the lab and must be collected from their native environment. They are collected from the top 6 cm of soil along with saline water. The water and soil mix is collected in buckets and stored in the lab at room temperature.

The data collection was done primarily as videos under a microscope with magnifications ranging from 20x to 60x. In order to get good images that could be analyzed with our tracking algorithm, the samples had to be cleaned. To do so, a small sample of about 100ml of mud and water was placed in a flask and a small neodymium magnet was placed outside, about 20mm away from one of the sides of the glass and 1cm above the soil. The mix of soil and water was stirred and allowed to settle. After approximately 20 minutes, 2 ml of water were sampled from the area surrounding the magnet and placed in a small vial. The process was then repeated with the smaller vial. After another 20 minutes, 40 μm were collected to put in slides or PDMS chambers.

After the purification of the samples and the video recording, the data were analyzed. The data analysis was done in Matlab. This process is explained in the Image processing and video analysis subsection of the Materials & Methods section.

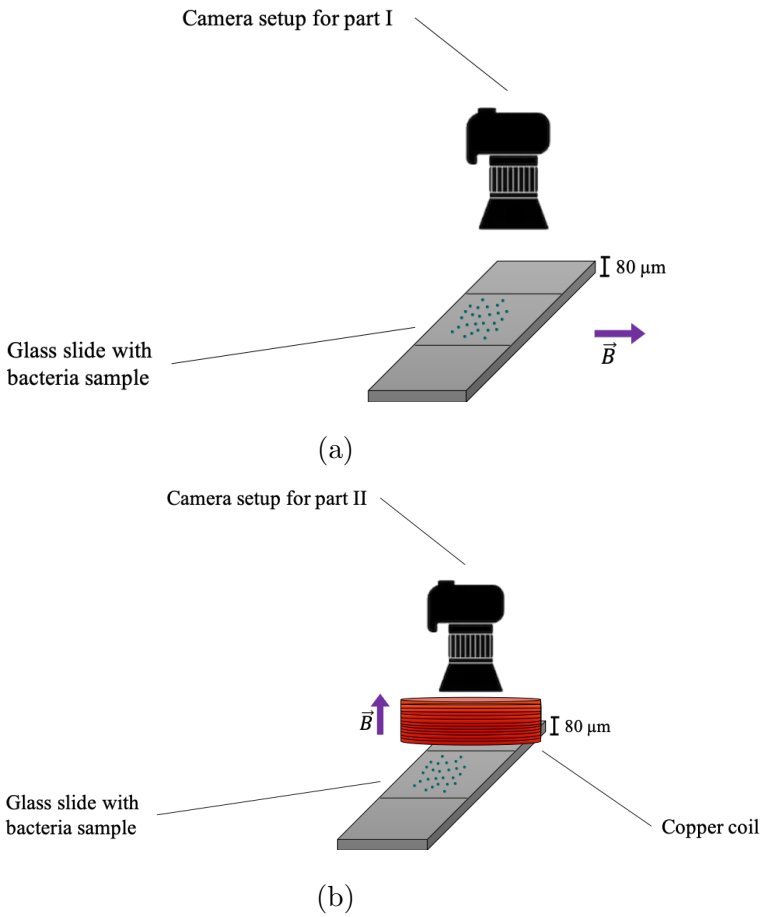

FIG. 2: (a) Experimental setup for first set of experiments where the magnetic field is pointed along the plane of the slide. (b) Experimental setup for second set of experiments where the magnetic field is pointed away from the plane of the slide and into the camera.

Two different sets of experiments were performed. The first set of experiments consisted of observing the bacteria swim along the slide with the magnetic field pointed along the plane of the slide. The second set of experiments was performed with the magnetic field pointed away from the plane and into the optical piece of the camera. The two experimental setups are illustrated in Figure 2.

Glass slides and microfluidic chambers

Throughout the experiments, we designed and built microfluidic chambers that would adjust to the different experimental designs. The microfluidic chambers were made out of Polydimethylsiloxane (PDMS). PDMS is a optically clear, silicon-based polymer. The

designs were made by using a photorestist over a silicon wafer. When exposing it to a UV light, the desired design stuck to the wafer and the unexposed photoresist was disolved. These silicon wafers served as the molds for the PDMS microfluidic chambers. The chambers designed had a depth of 50-100 μm. The chambers were bound to a glass slide by the method of plasma cleaning.

Image processing and video analysis

The image processing and video analysis was done in Matlab. The first step was to obtain a clear image. To do that, we deleted the background. The method we chose in order to delete the background was to average an image across the frames of the video. Then this average image was subtracted from each individual frame. This way, anything that was static throughout the video would be deleted. The next step was to detect the cells. We used a convolution filter to do so. Our convolution filter had the same average radius of the cells and was dark on the edges and light in the middle. By using a convolution on the frames of the video, any object that had the same size and features as our filter would get emphasized and everything else would get averaged.

Once the video frames had been processed, we used the Matlab function to find circles in order to detect the cells. This function allowed us to control the range of the radii we were interested in and how close to a perfect circle our cells had to be. We played with this numbers to find a spot where enough cells were being detected without too many false positives. To clean these detections, we then deleted the circles that would encompass other smaller circles and those that significantly overlapped.

After detecting the cells in the individual frames, we worked on tracking them from one frame to the next. We predicted where a cell would be based on their size and velocity. Then we assigned weights to the detected cells based on this predictions. These weights allowed us to connect one detection to the next based on probability and thus creating tracks. We used the individual frame detections when we wanted to analyze distributions and concentrations and we used the tracks to analyze the movement and dynamics of the MMB.

RESULTS

Having developed techniques to enrich MMB, we began our study of their dynamics. We first worked on confining them. The MMB were placed in a microfluidic chamber with a straight wall. The slide and camera setup were situated at the middle of a tri-axial Helmholtz coil system in order to have a uniform magnetic field. The magnetic field was then aligned to point along the plane of the slide and perpendicular to the microfluidic wall. This allowed us to observe the ping-pong behavior of the bacteria as the swam into the chamber's wall and bounced around back and forth.

We observed a distribution of bacteria in which there was a higher concentration closer to the wall and a lower concentration as we moved away from it. As the imposed magnetic field was increased, the bacteria were confined to a narrower portion of the slide, clumping more against the wall of the microfluidic chamber. We measured the number of occurrences at a gives distance from the wall up to 1000 μm for the different magnetic fields, which can be seen in Figure 3. We see that the general trend lines are straight on a logarithmic scale, which means that the decay is exponential as we move away from the wall. We can also see a trend as we increase the magnetic field. For weaker magnetic fields (in blue) the slope of the line is more horizontal, which means that as we go away from the wall, we find a lower but similar number of bacteria. As the magnetic field increases, the distribution steepens. In the higher magnetic fields (orange and red) the number of occurrences quickly drops. This follows our observations of higher concentrations near the wall for higher applied magnetic fields.

Using these observations, we were able to calculate an analogy to light's penetration depth. At the edge of the wall we find the highest concentration of cells. We see that the line fits our data well for 600 μm. We calculated the distance from the wall at which the concentration of bacteria dropped to $1/e$ (or about 37%) of the initial concentration. This value was calculated for the different magnetic fields and the plot can be seen in part (b) of Figure 3. The graph shows an increasing trend. As the inverse current increases, the imposed magnetic field decreases and the bacteria are less concentrated closer to the wall. A bigger penetration depth means that we still find a significant number of cells at a larger distance from the wall. For the weakest magnetic field, the concentration of cells dropped to $1/e$ after 300 μm while for the strongest magnetic field it took only 100 μm.

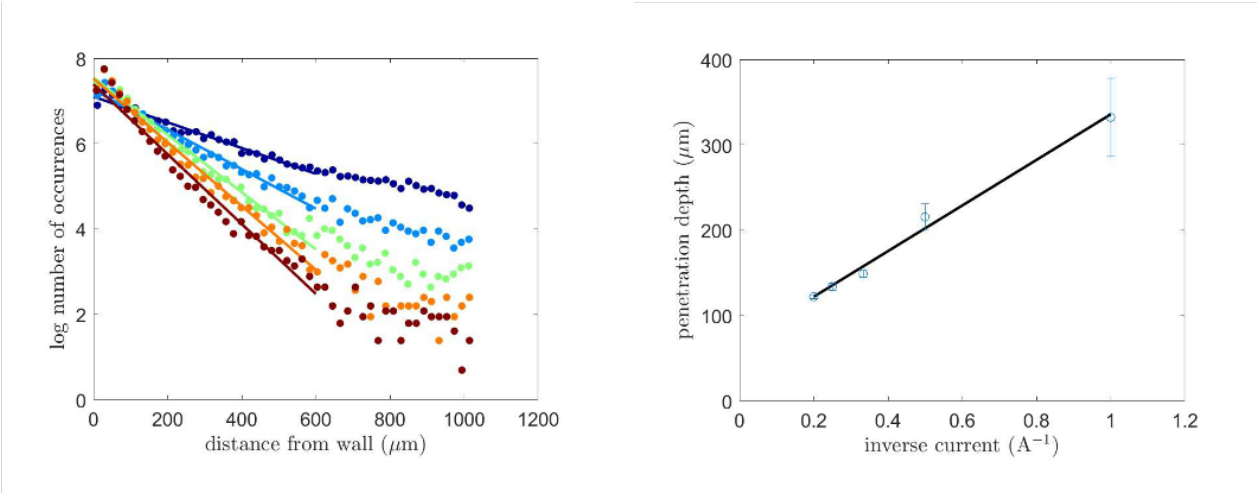

(a) (b)

FIG. 3: (a) The logarithm of the number of occurrences of bacteria as a function of distance from the wall for decreasing magnetic fields. (b) Calculated value of the penetration depth of the MMB colonies

After observing the behavior of the bacteria concentrating and bouncing along the flat wall, we proceeded to change our experimental setup to observe this behavior from a different angle. For this set of experiments, we used a copper coil around the eyepiece of the microscope (as illustrated on Figure 2 (b)) to induce a magnetic field that pointed away from the plane of the slide and directly towards the camera. We observed that the bacteria would swim into the slide. When they collided against the glass slide, they would spin around for some time, move along the slide and sometimes fade into the background. As predicted, we observed a higher concentration of bacteria when we imposed a greater magnetic field. The concentration was such that we observed colonies colliding into one another and forming a two dimensional layer. The MMB are being directed to swim towards the glass slide, but the glass slide becomes analogous to an obstacle. The behavior we are observing of ping-ponging into the background and swimming in circles might be the way they behave in nature to avoid obstacles during magnetotaxis.

The first measurements that we made were the instantaneous velocities of the individual cells that were swimming into the glass slide. We differentiated the cells that were swimming into the glass slide from those swimming along the glass slide by their type of motion. When bacteria were confined to the glass slide, they would move in a circular motion, instead of

traveling across the screen. This method was a good basic approach but it yielded a lot of false negatives. Many cells that were bound to the glass slide got ignored by our algorithm. We still decided to go for this method because it did a good job at ignoring the cells that were swimming quickly in the background and those would throw off our data analysis.

The instantaneous velocities were calculated by finding the displacement of each one of the cells from one frame to the next. The histogram for the velocities can be observed in Figure 4 (b). In this figure we can see how the peak for all of the different magnetic fields is around zero. This coincides with the observed behavior, as the cells that were swimming into the slide would barely move across the plane of the screen. The symmetry of the plot shows us that there is no bias in the direction of movement of the bacteria. We can also observe a trend as we increase the magnetic field. For the case of the weaker magnetic fields, depicted in blue and green, we observe a linear decrease in the number of bacteria moving at higher velocities. This shows that the distribution of their instantaneous velocities falls exponentially. As the magnetic field is increased, we see that the absolute value of the slope increases. In the trials with the stronger magnetic fields, shown in red and dark red, the decrease is very sharp, which almost looks Gaussian. The peak is also higher for the stronger magnetic fields. This means that we have more bacteria moving at zero velocity, and the number of bacteria quickly drops as the absolute value of the velocity increases.

These observations can be tied to two behaviors. One of them is the confinement of the cells to the glass slide. In the first part of the experiment, we observed that at higher magnetic fields, the bacteria were found closer to the wall. This would confine them to the glass slide strongly. The strength in the magnetic field would cause the bacteria to bind to the glass slide regardless of the angle of approach or the velocity at it which it collided with the glass slide. The magnetic field would then create a stable fixed point which MMB would reach when they collided against the wall. Another behavior that is probably a cause for this distribution of instantaneous velocities is the increase of density and form of arrangement as the magnetic field is increased. In Figure 4 (a), we can see a frame of the video at a weak magnetic field and at a strong magnetic field. At a low magnetic field, there is a low density of bacteria, so the distance between colonies is greater than the average diameter. In the case of the stronger magnetic field, we can see that there is a higher density of bacteria. The distance between MMB colonies decreases, and the majority of cells have close neighbors within a distance of a body length. The behavior of an individual cell colony is now greatly

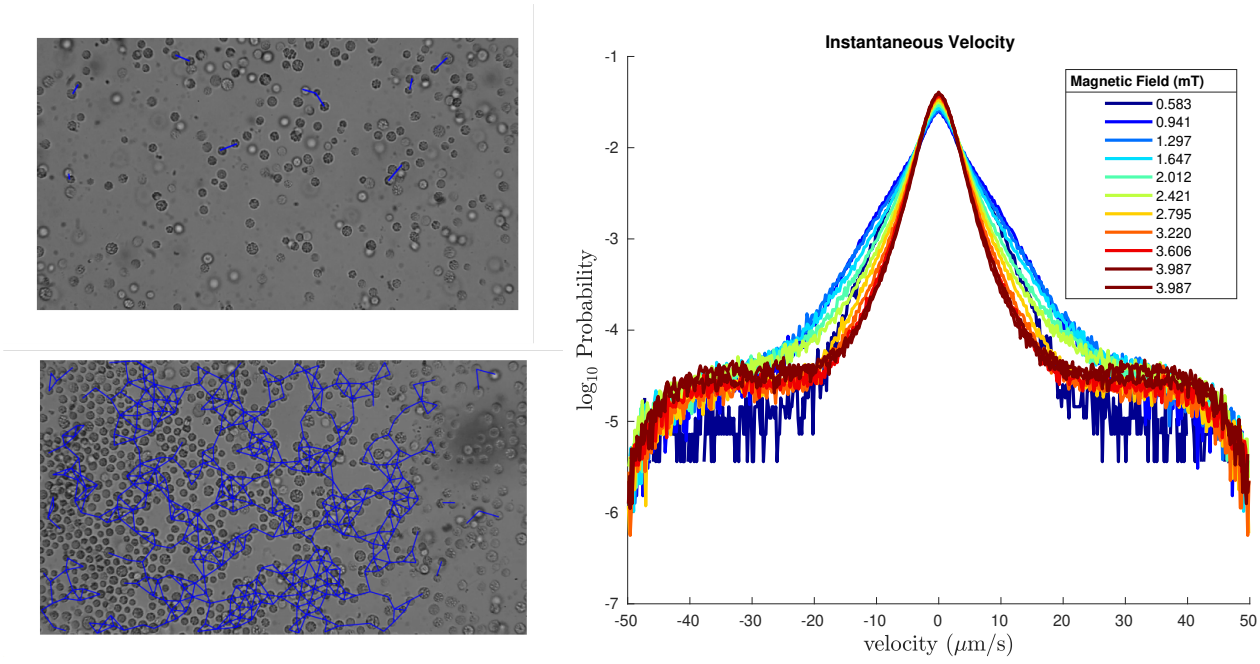

(a) (b)

FIG. 4: (a) Distribution of MMB colonies at low magnetic field vs high magnetic field. The blue lines represent the cells less than a body length apart from one another. (b) Histogram of the distribution of instantaneous velocities of MMB subject to different applied magnetic fields.

affected by the other colonies around it. They are all bumping into one another which limits their overall ability to move. The blue lines in both of the frames show the detected cells that are within 1.05 body lengths of each other, so the colonies that are basically touching one another. This allowed us to observe the number of near neighbors and the overall distribution of the cells in the glass slide.

The distribution of MMB showed that there was cluster formation. As the magnetic field increased, the was a greater chance of cells to be in a cluster instead of free swimming. We wanted to analyze the formation of spanning clusters as we increased the magnetic field. We saw a trend as we increased the magnetic field. At low magnetic field and low density, most cells were free swimming but at high magnetic fields we had a big cluster with most of the cells in it. In order to calculate the ratio of the area of the biggest cluster to total area of the screen, we drew a convex hull around the edges of the cluster with the greatest number of MMB and calculated its area. This would allow us to get around some of the

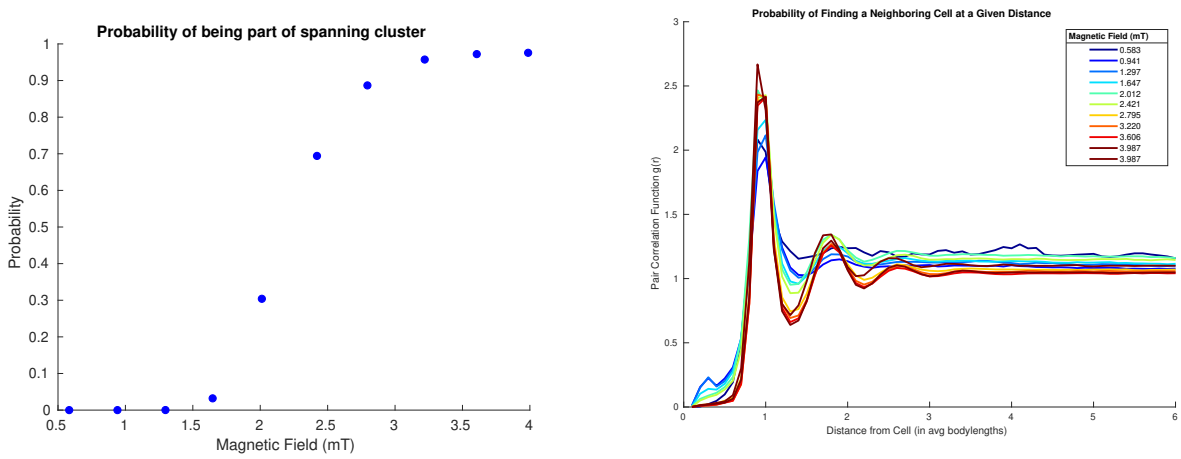

(a) (b)

FIG. 5: (a) Probability of a cell to be found within the spanning cluster as a function of applied magnetic field. (b) Pair correlation function $g(r)$ as a function of distance measured in body lengths for different magnetic fields.

false negative detections that our algorithm was ignoring. A convex hull around the edges of a cluster accounted for some of the cells inside that were not being detected or had been dropped out. This gave us a better idea of the actual size of the clusters. If the area of the convex hull was greater than half the total area of the screen, we would consider this a spanning cluster. For each frame, we calculated the presence of a spanning cluster. If there was a spanning cluster, we took the ratio of the cells in the biggest cluster to the total number of cells. We averaged this number throughout all frames at each magnetic field. At low magnetic field, there was no spanning cluster, and at a high magnetic field, almost all of the bacteria are found within the spanning cluster. We decided to see if there was such thing as a critical magnetic field by making this system analogous to a phase transition. In Figure 5 (a) we can see the probability of a colony to be within the spanning cluster as a function of magnetic field. For low magnetic fields, the probability is zero and it increases smoothly up to a probability of almost one for strong magnetic fields. The inflection point on this graph is at around 2.15 mT.

Following the analogy of the phase transition, the one dimensional system of bacteria looked like it could be an active crystal, a liquid crystal, or a gel. We calculated the pair correlation function of our system.

The pair correlation function is calculated by selecting a reference colony and measuring how many colonies are found at a distance r. In Figure 6 we can see the reference colony marked by a black dot. The colonies found in between the two black circles are the ones which are counted for the pair correlation. In Figure 5 (b) we can see the trend that the pair correlation function has. For distances less than one body length, it is pretty much zero. It is quite unlikely to find cells at this distance because the cells cannot occupy the same space. We would see some cases in which this would happen, for example when one cell was smaller than an average radius or when it was behind, almost forming a second layer over the main monolayer. Then, at one body length, we can see a sharp spike. This spike is more pronounces for the higher magnetic fields, but it is still there for low magnetic fields. This tells us that it is very likely to find cells that are basically side by side. In the case of the low magnetic fields, this can be explained by the presence of dipoles, and at higher magnetic fields by the close packing. We can see that there is another bump before two body lengths, three body lengths and even four body lengths. The bumps are more pronounced as the magnetic field increases and nonexistent for low magnetic fields. This shows us that at strong magnetic fields, the colonies are strongly correlated with one another. The bacteria are behaving as incompressible spheres at short range.

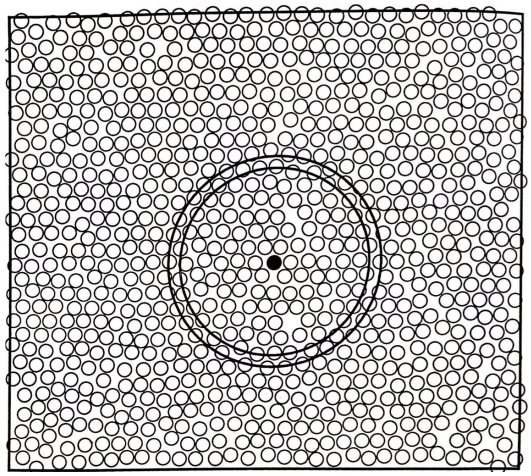

FIG. 6: Calculation of the pair correlation function

CONCLUSIONS

In this project, we studied a biological system in which we had partial control of the individual motion of the bacteria colonies. This allowed us to play with the bacteria and study them in a diversity of set ups. We saw how an increase in magnetic field directly affected the organization of the system by increasing the concentration of cells against a wall. The individual cells had a ping-ponging behavior in which they spontaneously reversed

their direction and swam anti-parallel to the magnetic field. The behavior of the system transitioned from a group of free swimming fast bacteria to a system with a crystaline packing and little motion as we increased the magnetic field. At a high magnetic field along the wall, the system formed a mono-layer. This two dimensional layer of MMB colonies behaved like an active crystal in which individuals randomly detached and reincorporated.

[1] F. Abreu, J. L. Martins, T. S. Silveira, C. N. Keim, H. G. P. L. de Barros, F. J. G. Filho, and U. Lins, International Journal of Systematic and Evolutionary Microbiology **57**, 1318–1322 (2007).

[2] S. L. Simmons and K. J. Edwards, Environmental Microbiology **9**, 206–215 (2007).

[3] S. Spring and D. A. Bazylinski, Prokaryote **13**, 842–862 (2006).

[4] D. A. Bazylinski and R. B. Frankel, Nature Reviews, Microbiology **2**, 217–230 (2002).